Supporting Information

Multisegmented hybrid-polymer based on oligo-amino acids: synthesis and secondary structure in solution and the solid state

Jan Freudenberg[a] *and Wolfgang H. Binder**[a]

a. Martin Luther University Halle-Wittenberg, Faculty of Natural Sciences II, Chair of Macromolecular Chemistry, D-06120 Halle

Content

Synthesis of N-carboxyanhydrides (NCA´s) 3
S1. ^{1}H-NMR spectra of NCAs 3
Synthesis of the initiator *10-undecene-1-amine* 4
Synthesis of 10-undecenecarboxamide 4
Synthesis of 10-undecene-1-amine 4
S2. ^{1}H-NMR spectra of initiator 4
S3- S4. FTIR investigation for ROP of NCA´s 5
S5. – S8. MALDI-TOF-MS of oligomers 7
S9. – S12. ^{1}H-NMR spectra of oligomers and corresponding ADMET-polymers 8
S13. – S16. Preparative GPC curves for the fractionated ADMET-polymers 11
S17. – S19. Analytical GPC curves for the fractionated ADMET-polymers 13
S20. WAXS-investigation of $O^{Bn}Glu_{10}$ and $AP_3(^{Bn}Glu_{10})$ 15
S21. – S23. FTIR in solid state for chosen fractions of $AP_m(^{Bn}Asp_3)$ and $AP_m(^{Bn}Asp_{10})$ 15
S24. CD measurement of oligomer $O^{Bn}Glu_{10}$ and polymer $AP_3(^{Bn}Glu_{10})$ (unfractionated) in HFIP-solution. 17

S25. – S28. Concentration dependent FTIR measurements of oligomers and corresponding ADMET-polymers (unfractionated) in HFIP-solution. 17

References 19

Synthesis of N-carboxyanhydrides (NCA´s)

The synthesis of *N*-carboxyanhydrides were done according to literature.[1] In a typical reaction the amino acid (5-10 g; 1.0 eq) and α-pinene (2.0 eq) were suspended in dry ethyl acetate (10 mL per 1.0 g amino acid) and heated up to 70°C. Triphosgene (0.5 eq) was dissolved in dry ethyl acetate (adjusting a concentration of 10 mmol mL^{-1}) and the resulting solution was added dropwise over a period of 10 min. The reaction was finished after the reaction mixture becomes clear. At this point the mixture was allowed to react for two more hours to remove excess triphosgene from the reaction. The resulting mixture was cooled to room temperature and residual HCl and phosgene were purged out with N_2 and trapped in an adsorption bottle filled with aqueous NaOH. The solvent was removed in vacuum and the crude product was recrystallized three times in ethyl acetate:*n*-hexane mixture (1:10), filtrated and dried in vacuum to yield the products as white powders (80-90%).

Glu-NCA: ^{1}H-NMR ($CDCl_3$, 27 °C, 400 MHz): δ [ppm] 2.12 (m, 1H, H_4), 2.28 (m, 1H, H_4), 2.59 (t, $^3J_{H,H}$ = 6.8 Hz, 2H, H_5), 4.37 (t, $^3J_{H,H}$ = 6.0 Hz, 1H, H_3), 5.14 (s, 2H, H_7), 6.48 (s, 1H, H_{14}), 7.31 – 7.45 (m, 5H, H_9 – H_{13}).

Asp-NCA: ^{1}H-NMR ($CDCl_3$, 27 °C, 400 MHz): δ [ppm] 2.88 (dd, $^3J_{H,H}$ = 17.8 Hz, $^2J_{H,H}$ = 4.3 Hz, 1H, H_4), 3.05 (dd, $^3J_{H,H}$ = 17.8 Hz, $^2J_{H,H}$ = 4.9 Hz, 1H, H_4), 4.67 (t, $^3J_{H,H}$ = 4.5 Hz, 1H, H_3), 5.12 (s, 2H, H_6), 6.15 (s, 1H, H_{13}), 7.31 – 7.45 (m, 5H, H_8 – H_{12}).

S1. ^{1}H-NMR spectra of NCAs

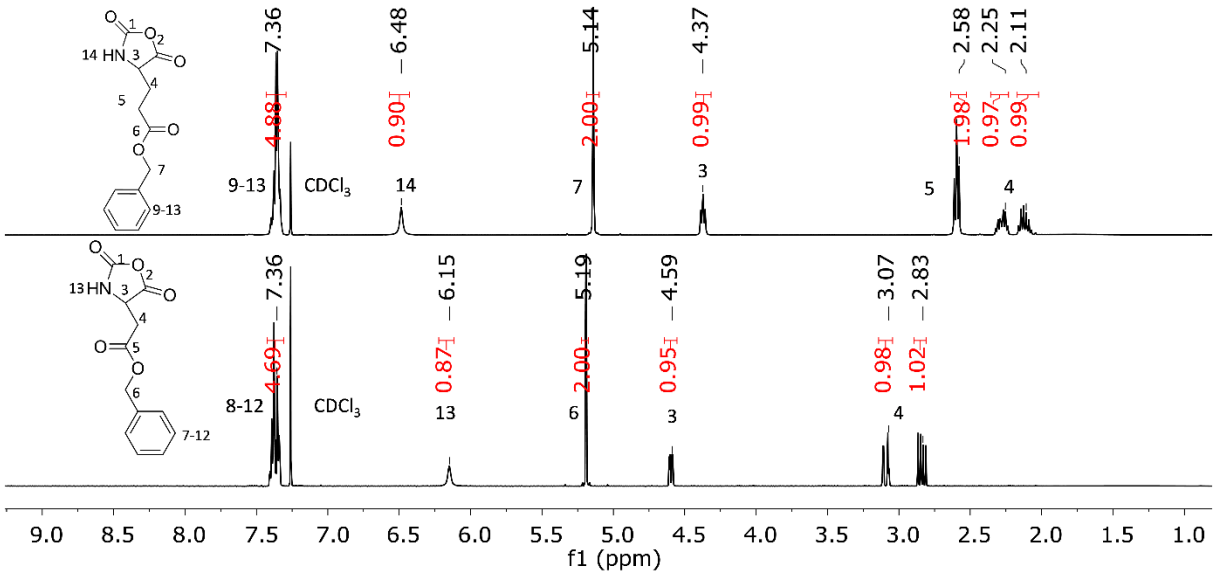

Figure S1. ^{1}H-NMR spectra of **Glu-NCA** (top) and **Asp-NCA** (bottom) in $CDCl_3$.

Synthesis of the initiator *10-undecene-1-amine*

Synthesis of 10-undecenecarboxamide

Synthesis of 10-undecenecarboxamide was done according to literature.[1] In a two necked round bottom flask, equipped with a magnetic stirrer, a solution of aqueous ammonium hydroxide (250 mL) was added and cooled to 0°C. 10-Undecenoyl chloride (12.69 g; 0.06 mol; 1 eq) was dissolved in THF (50 mL) and added dropwise to the solution, which was allowed to stir at room temperature for 3h. The solid product was filtered off, washed with distilled water (3x100 mL) and dried under vacuum to yield 10.85 g (95 %) of 10-undecencarboxamide.

^{1}H-NMR ($CDCl_3$, 27 °C, 400 MHz): δ [ppm] 1.29 – 1.38 (m, 10H, H_d –H_h), 1.63 (m, 2H, H_i), 2.05 (m, 2H, H_c), 3.25 (t, $^3J_{H,H}$ = 7,0 Hz, 2H, H_j), 4.96 (m, 2H, H_a), 5.83 (m, 1H, H_b).

Synthesis of 10-undecene-1-amine

Synthesis of 10-undecene-1-amine was done according to literature.[1] In an inert atmosphere $LiAlH_4$ (6.50 g; 171.3 mmol; 2.9 eq) was suspended in dry THF (150 mL), cooled to 0 °C and 10-undecenecarboxamide (10.85 g; 59.2 mmol; 1.0 eq) dissolved in dry THF (150 mL) was added dropwise to the solution. The mixture was allowed to stir at room temperature for 24h, cooled afterwards to 0 °C and was quenched carefully by adding water (20 mL), 1M NaOH-solution (40 mL) and water (20 mL). The mixture was filtered and the filtrate was concentrated in vacuum obtaining the crude product, which was dissolved in diethyl ether (50 mL) and washed with brine (2x100 mL). The organic layer was dried over Na_2SO_4, and purified finally by high vacuum distillation (30 – 38 °C at 0.032 mbar) to yield 5.52 g (55%) of 10-undecene-1-amine.

^{1}H-NMR ($CDCl_3$, 27 °C, 400 MHz): δ [ppm] 1.05 – 1.39 (m, 14H, H_d – H_j), 2.01 (m, 1H, H_c), 2.65 (t, $^3J_{H,H}$ = 7.0 Hz, 1H, H_k), 4.95 (m, 1H, H_a), 5,80 (m, 2H, H_b).

S2. ^{1}H-NMR spectra of initiator

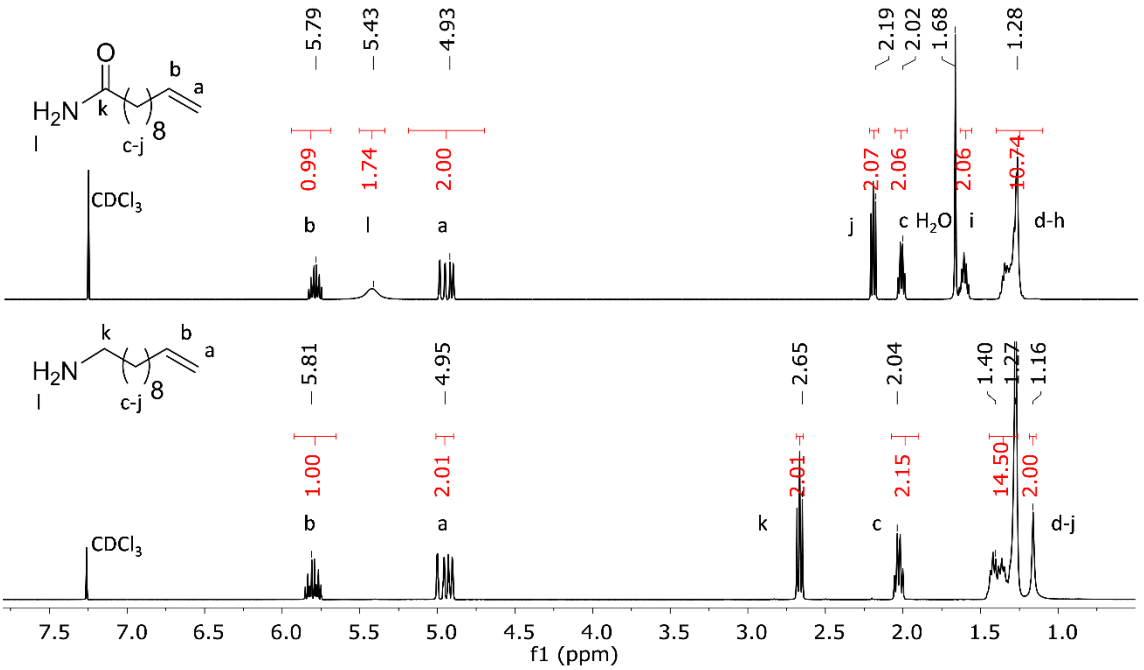

Figure S2. ^{1}H-NMR spectra of 10-undecenecarboxamide (top) and 10-undecene-1-amine (bottom) in $CDCl_3$.

S3- S4. FTIR investigation for ROP of NCA´s

FTIR spectroscopic investigation for the synthesis of oligomeric $O^{Bn}Glu_{10}$ (see Figure S3) and for $O^{Bn}Asp_{10}$ (see Figure S4): starting from the spectra of the virgin **Glu-NCA** or **Asp-NCA** in DMF without the amine initiator as reference value (t=0 min, black curve) a stepwise decrease in intensity of the NCA-vibration band at 1785 cm^{-1} and 1854 cm^{-1} was observed after adding the initiator. After 70 minutes for **Glu-NCA** (Figure S3 pink curve) and 450 minutes for **Asp-NCA** (Figure S4 brown curve) both signals had completely disappeared, indicating the complete conversion of the monomer.

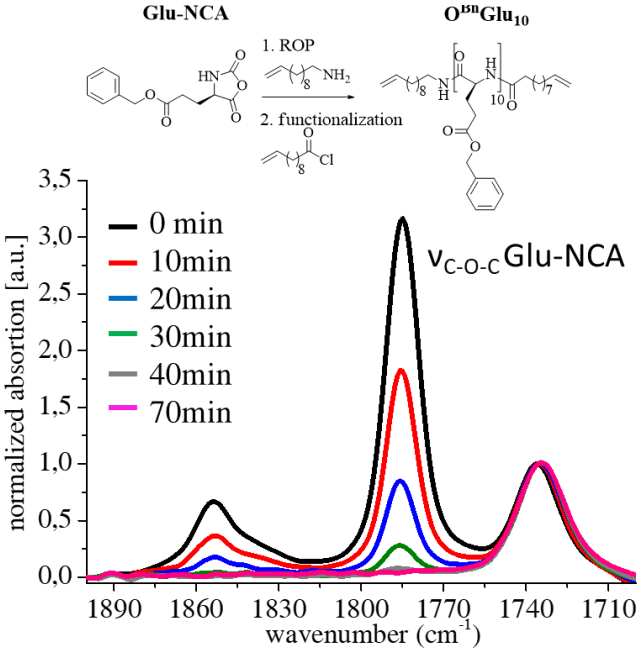

Figure S3. Following of the stepwise NCA-consumption during ROP of **Glu-NCA** to **O^{Bn}Glu$_{10}$** by FTIR investigation of NCA C-O-C anhydride vibration band at 1785 cm^{-1} and 1854 cm^{-1} (spectra is normalized to the absorption band of benzyl group at 1735 cm^{-1}).

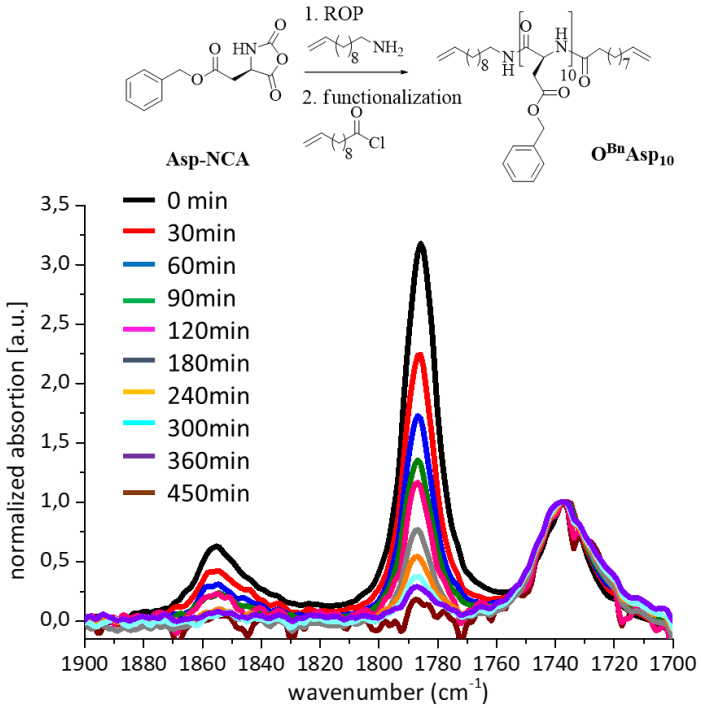

Figure S4. Following of the stepwise NCA-consumption during ROP of **Asp-NCA** to **O^{Bn}Asp$_{10}$** by FTIR investigation of NCA C-O-C anhydride vibration band at 1785 cm^{-1} and 1854 cm^{-1} (spectra is normalized to the absorption band of benzyl group at 1735 cm^{-1}).

S5. – S8. MALDI-TOF-MS of oligomers

MALDI-TOF-MS of e.g. **O^{Bn}Glu$_3$** (Figure S5) proved the structure as determined by one main series with a distance between the signals of 219 Da and a maximum peak of 1250.777 Da which was simulated to 1250.640 Da for $C_{130}H_{158}N_{10}O_{28}K^+$.

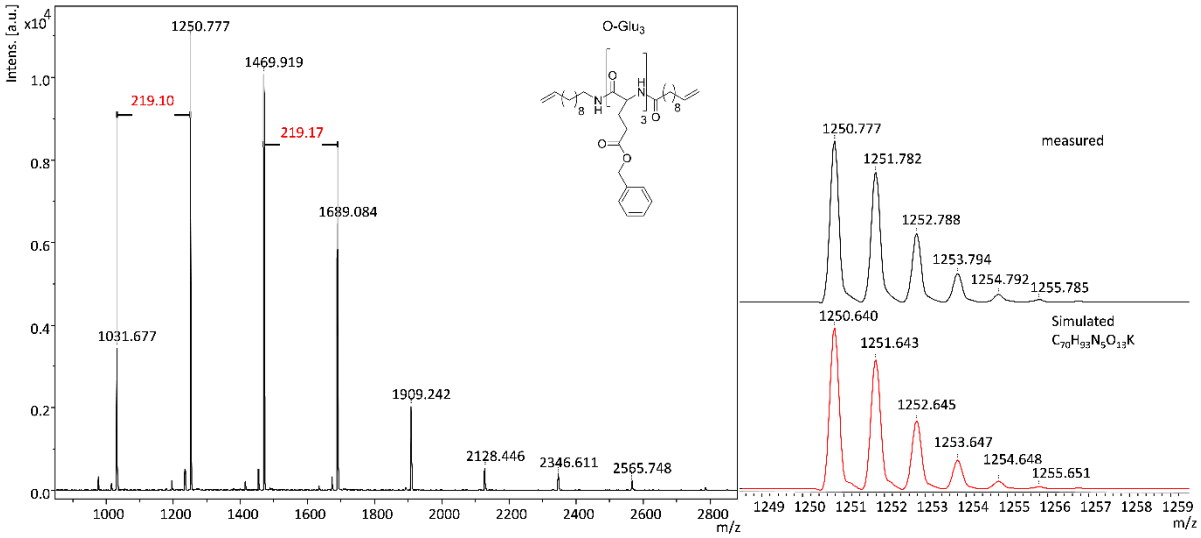

Figure S5. MALDI-TOF-MS of **O^{Bn}Glu$_3$** using dithranol as matrix and KTFA as salt.

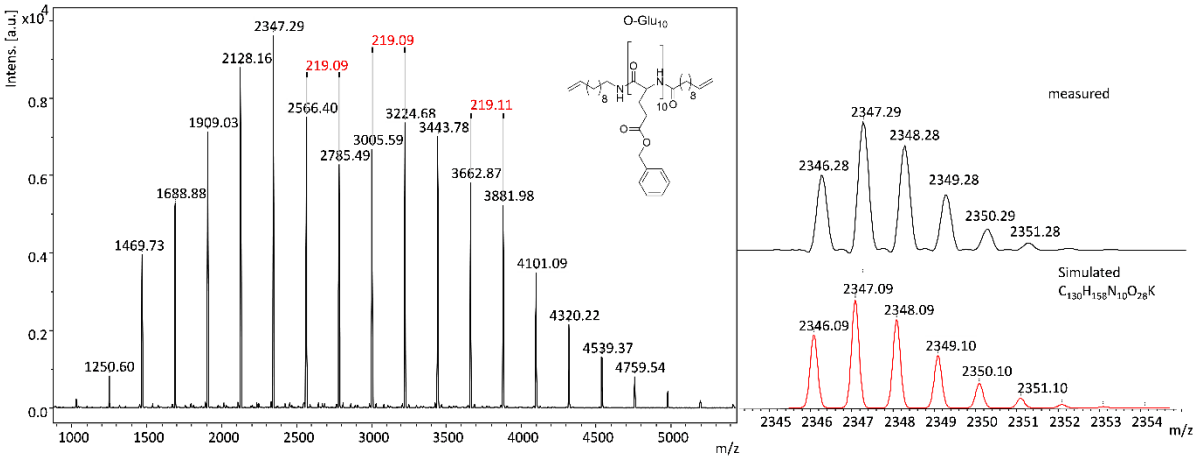

Figure S6. MALDI-TOF-MS of **O^{Bn}Glu$_{10}$** using dithranol as matrix and KTFA as salt.

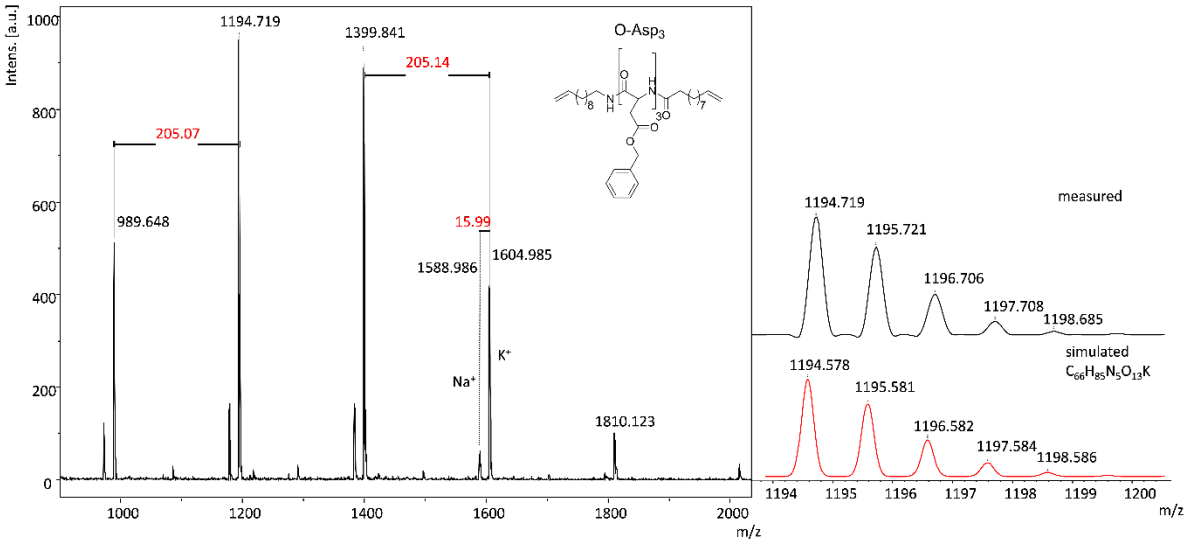

Figure S7. MALDI-TOF-MS of $\mathbf{O^{Bn}Asp_3}$ using dithranol as matrix and KTFA as salt.

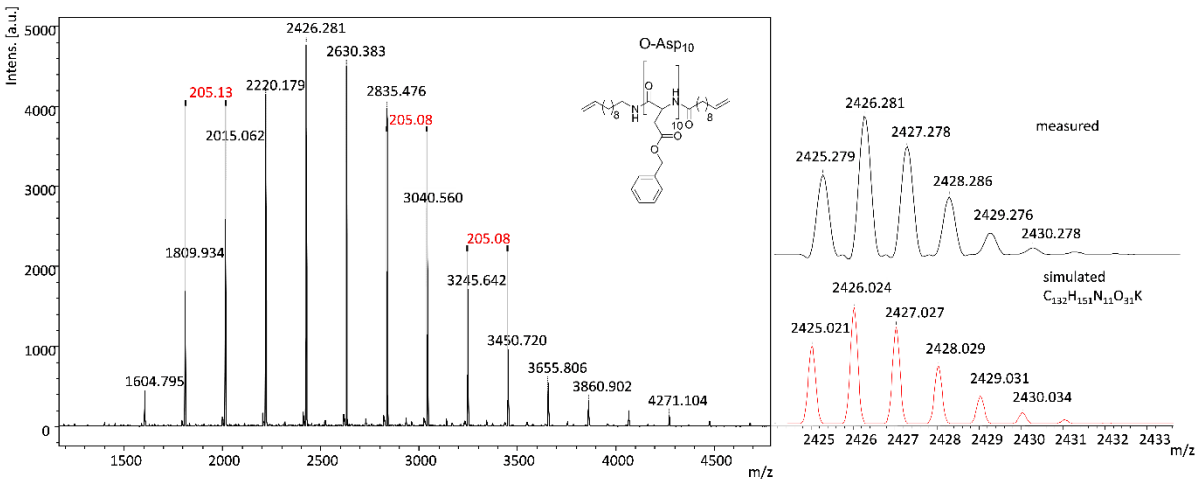

Figure S8. MALDI-TOF-MS of $\mathbf{O^{Bn}Asp_{10}}$ using dithranol as matrix and KTFA as salt.

S9. – S12. ^{1}H-NMR spectra of oligomers and corresponding ADMET-polymers

Selected ^{1}H-NMR spectra for $\mathbf{O^{Bn}Glu_3}$ (top) and $\mathbf{AP_{21}(^{Bn}Glu_3)}$ (bottom) are shown in Figure S9 revealing (eg. for $\mathbf{O^{Bn}Glu_3}$) characteristic signals of the C_α-proton (H_1) at 4.01 ppm – 4.27 ppm for the repetitive amino acid units in the main chain, as well as the aromatic protons (H_6 – H_{11}) at 7.32 ppm in the side chain. The successful attachment of the initiator and modification of the *N*-terminus can be proven by the characteristic signals for the CH_2-group next to the amide bonds (H_p + H_j) at 2.12 ppm and 3.04 ppm as well as the characteristic signals for the

vinyl protons (H_a + H_b) at 4.94 ppm and 5.75 ppm. The molecular weight of the oligomer could be calculated *via* ^{1}H-NMR by using the vinyl protons as reference, determined as 1,05 kDa *via* ^{1}H-NMR and is comparable to the molecular weight of 0,92 kDa determined by GPC. These vinyl protons are no longer visible after ADMET-polymerization caused by the high molecular weight of **AP$_{21}$(^{Bn}Glu$_3$)** and the new signal for the protons of the internal double bond at 5.31 ppm clearly identify the successful metathesis reaction (Figure S9 bottom).

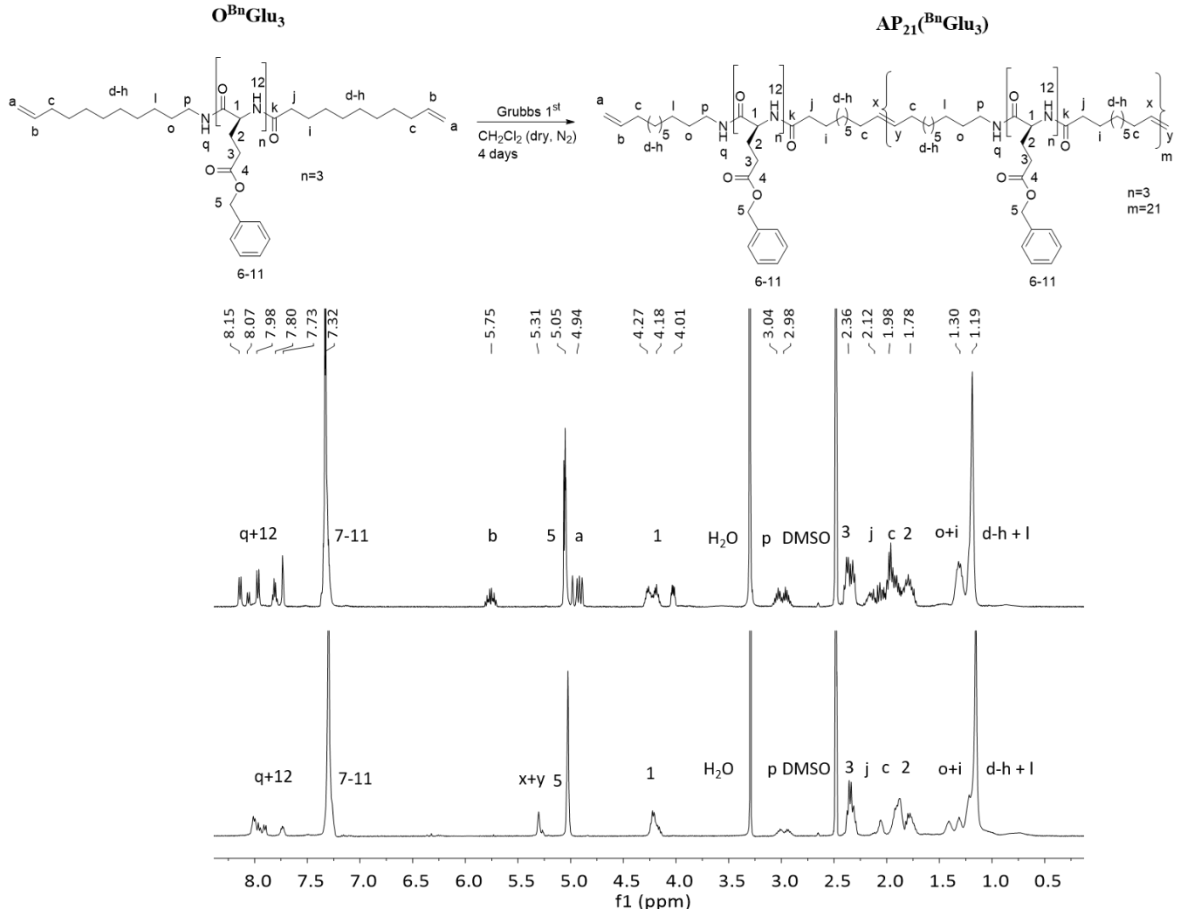

Figure S9. ^{1}H-NMR spectra of **O^{Bn}Glu$_3$** (top) and **AP$_{21}$(^{Bn}Glu$_3$)** (bottom).

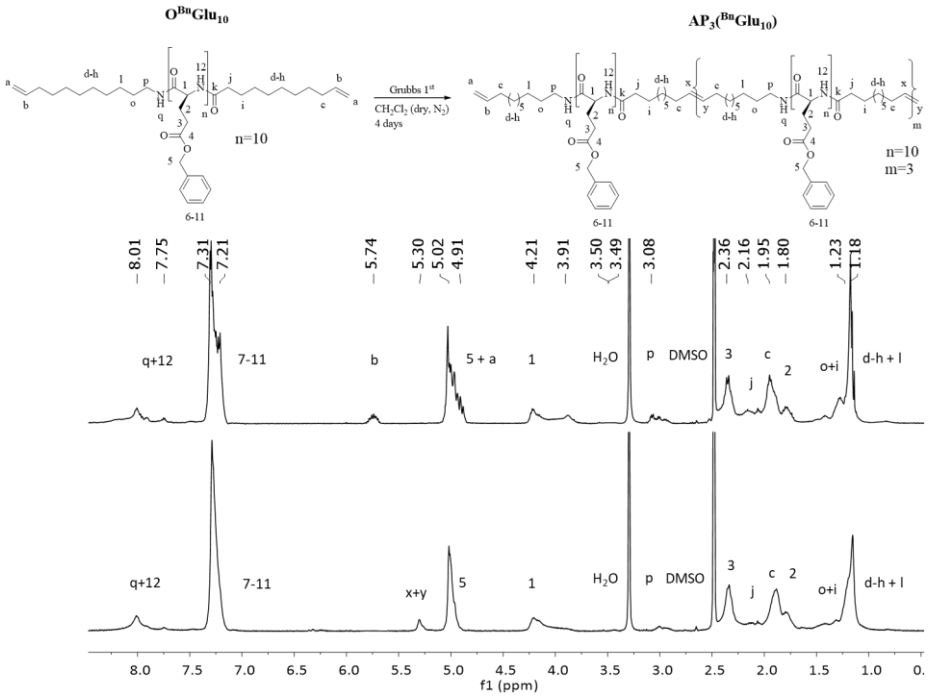

Figure S10. ^{1}H-NMR spectra of **O^{Bn}Glu$_{10}$** (top) and **AP$_3$(^{Bn}Glu$_{10}$)** (bottom).

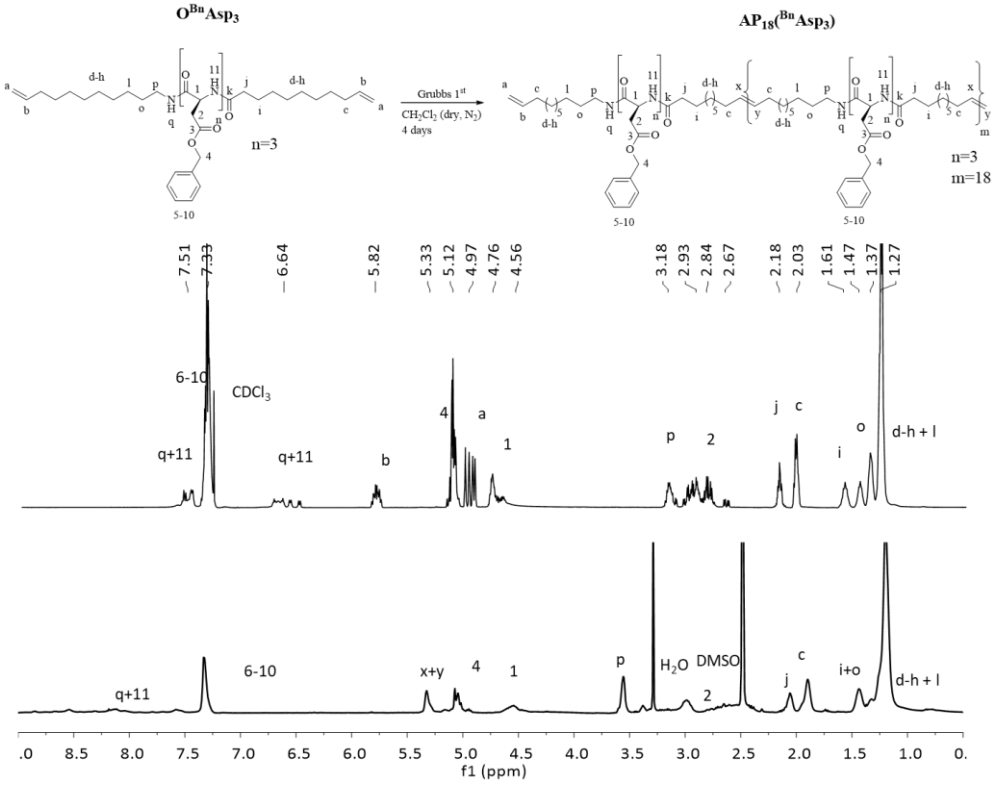

Figure S11. ^{1}H-NMR spectra of **O^{Bn}Asp$_3$** (top) and **AP$_{18}$(^{Bn}Asp$_3$)** (bottom).

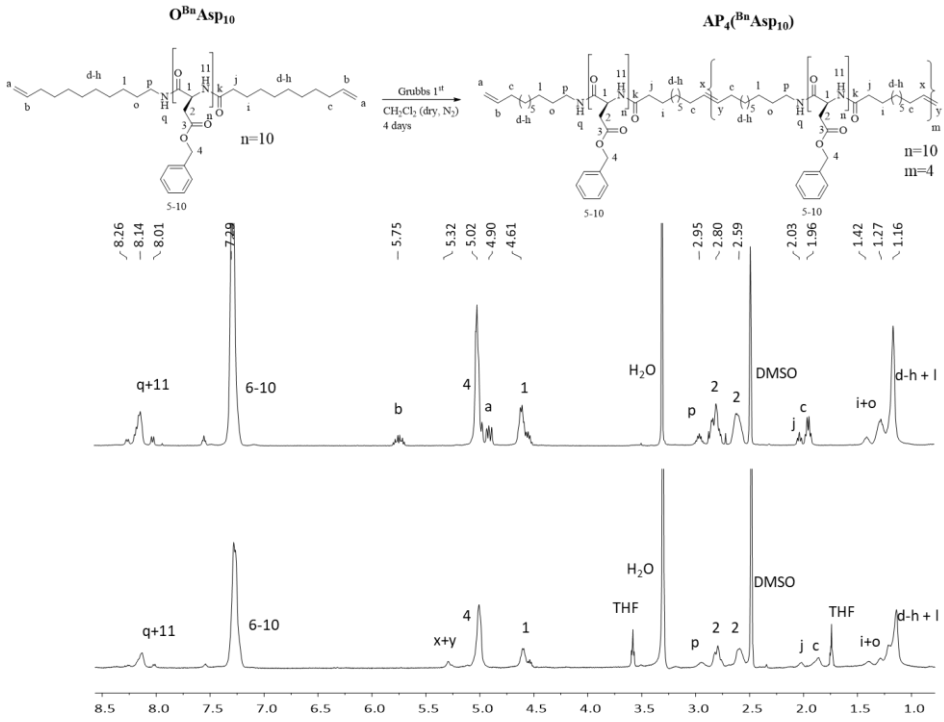

Figure S12. ^{1}H-NMR spectra of **O^{Bn}Asp$_{10}$** (top) and **AP$_4$(^{Bn}Asp$_{10}$)** (bottom). **AP$_4$(^{Bn}Asp$_{10}$)** was dried in high vacuum for one more day to remove rests of THF.

S13. – S16. Preparative GPC curves for the fractionated ADMET-polymers

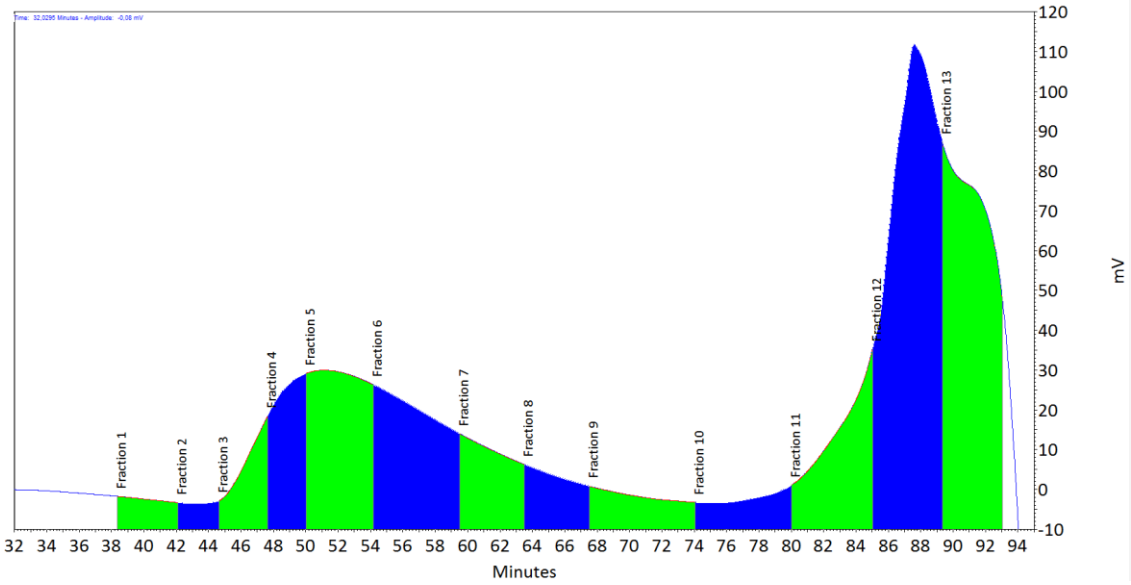

Figure S13. Preparative GPC curve for fractionation of **AP$_{21}$(^{Bn}Glu$_3$)** in DMF (for fraction 1+2 no polymer could be obtained, for detailed information see table 1.).

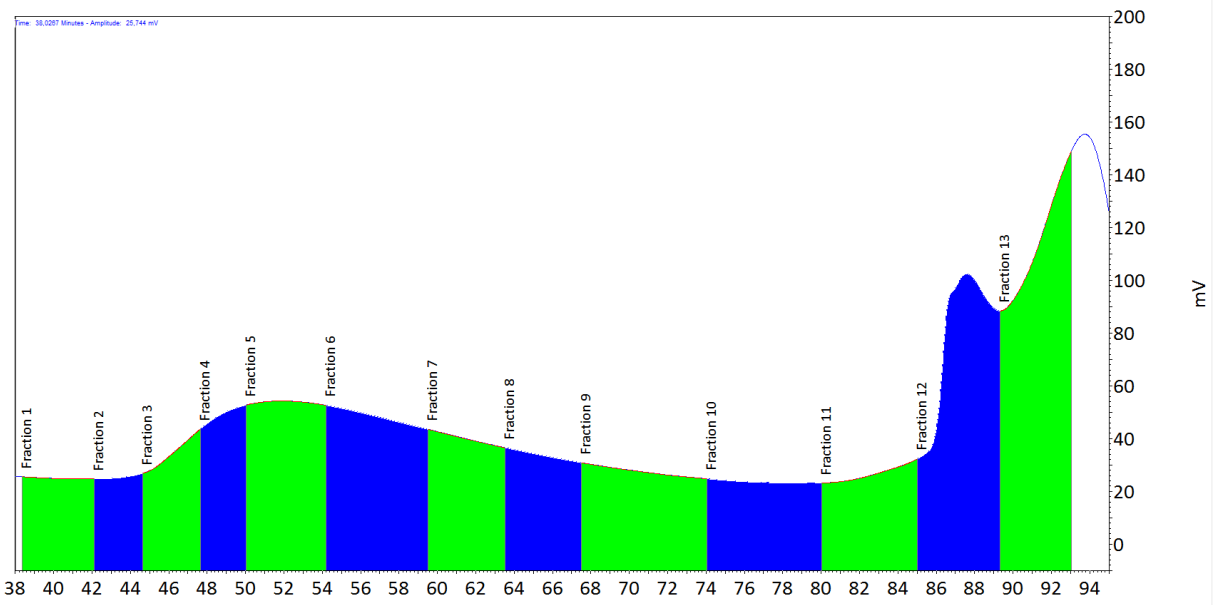

Figure S14. Preparative GPC curve for fractionation of **AP$_3$(^{Bn}Glu$_{10}$)** in DMF (for fraction 1+2 no polymer could be obtained, for detailed information see table 1.).

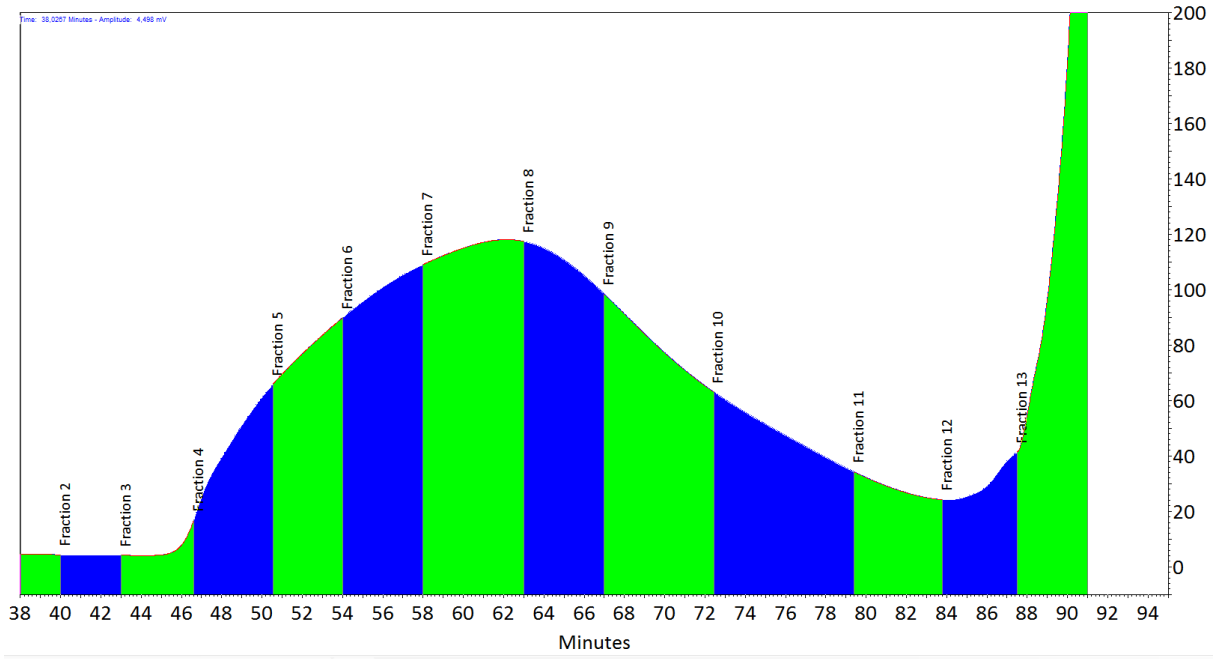

Figure S15. Preparative GPC curve for fractionation of **AP$_{18}$(^{Bn}Asp$_3$)** in DMF (for fraction 1+2 no polymer could be obtained, for detailed information see table 1.).

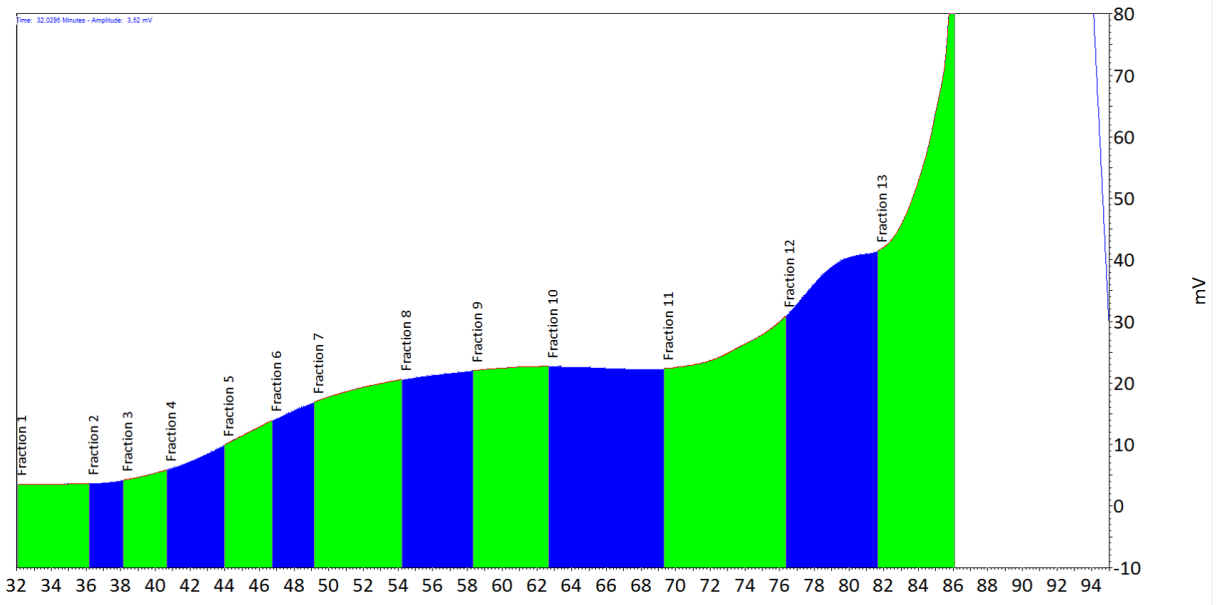

Figure S16. Preparative GPC curve for fractionation of **AP$_4$(^{Bn}Asp$_{10}$)** in DMF (for fraction 1+2 no polymer could be obtained, for detailed information see table 1.).

S17. – S19. Analytical GPC curves for the fractionated ADMET-polymers

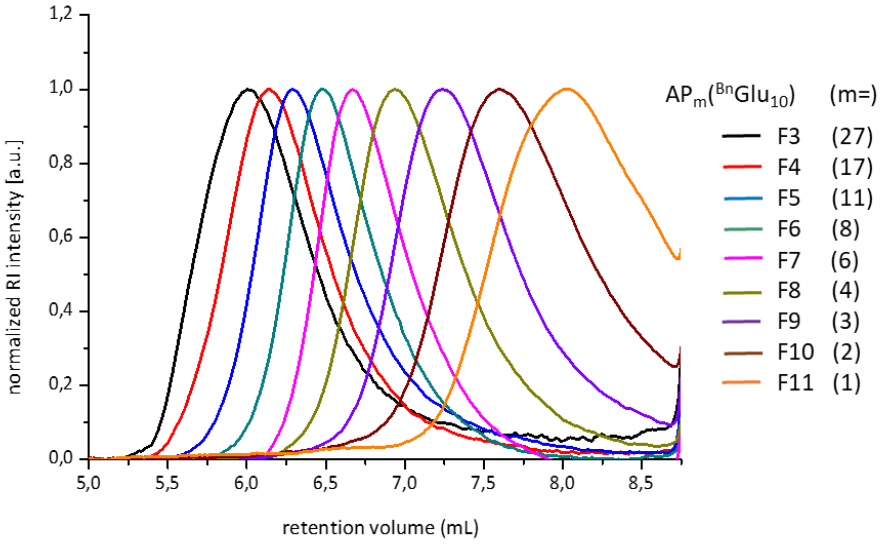

Figure S17. Normalized analytical GPC curves for obtained fractions of **AP$_3$(^{Bn}Glu$_{10}$)** after separation by prep. GPC.

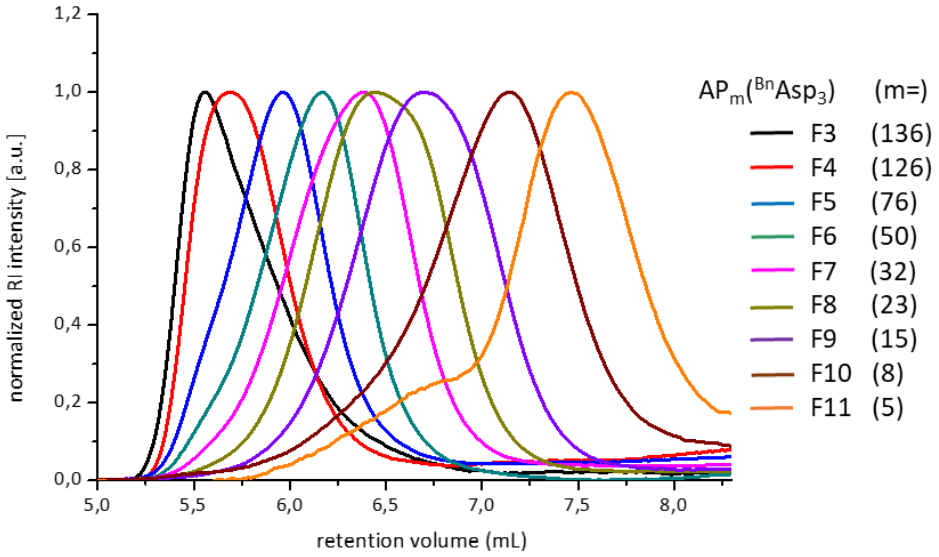

Figure S18. Normalized analytical GPC curves for obtained fractions of **AP$_{18}$(^{Bn}Asp$_3$)** after separation by prep. GPC.

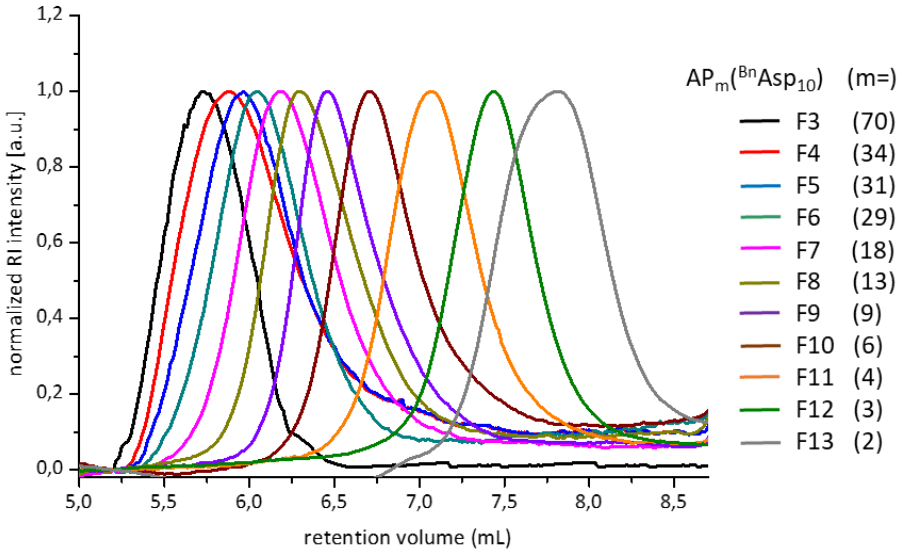

Figure S19. Normalized analytical GPC curves for obtained fractions of **AP$_4$(^{Bn}Asp$_{10}$)** after separation by prep. GPC.

S20. WAXS-investigation of $O^{Bn}Glu_{10}$ and $AP_3(^{Bn}Glu_{10})$

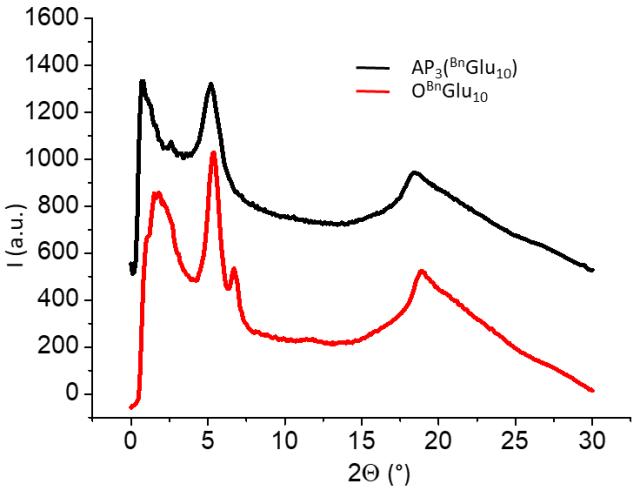

Figure S20. Wide-angle-X-ray diffraction patterns for **$O^{Bn}Glu_{10}$** (red) and **$AP_3(^{Bn}Glu_{10})$** (black).

S21. – S23. FTIR in solid state for chosen fractions of $AP_m(^{Bn}Asp_3)$ and $AP_m(^{Bn}Asp_{10})$

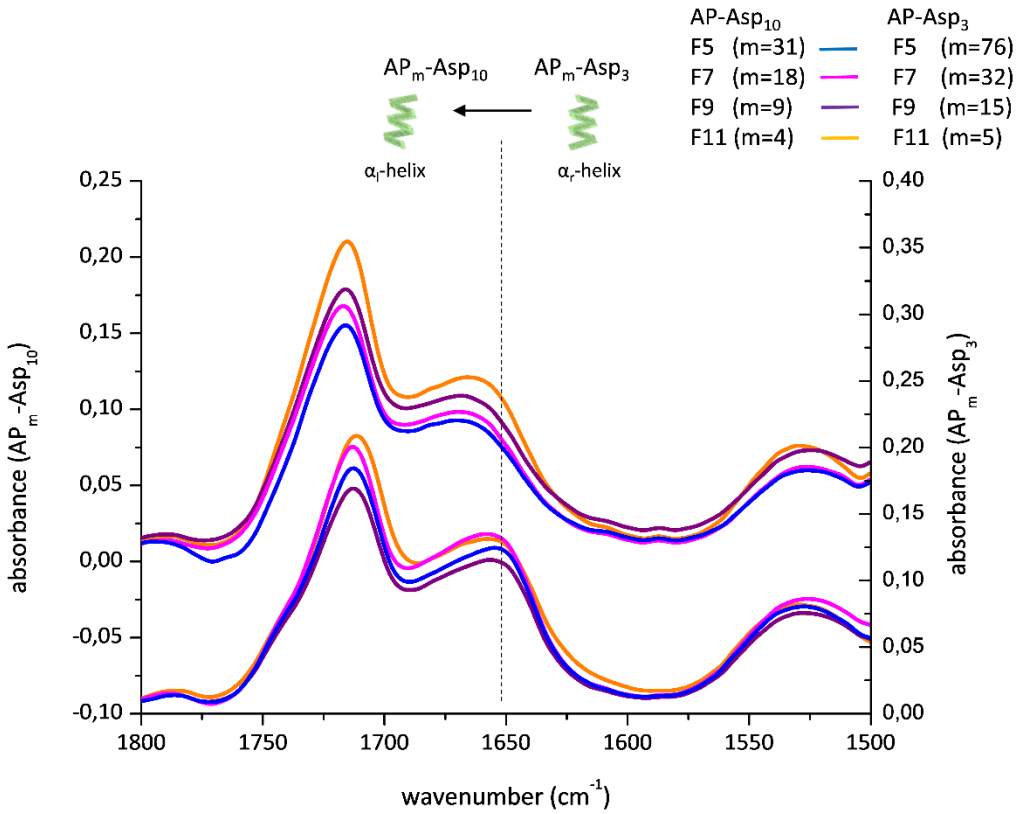

Figure S21. Solid state FTIR spectra for chosen fractions of **$AP_m(^{Bn}Asp_{10})$** (top) and **$AP_m(^{Bn}Asp_3)$** (bottom). No significant changes for different molecular weights (fractions) of the same ADMET-

polymer could be observed, but a transition from right handed to left handed helical screw sense for increasing number of amino acids per building block.

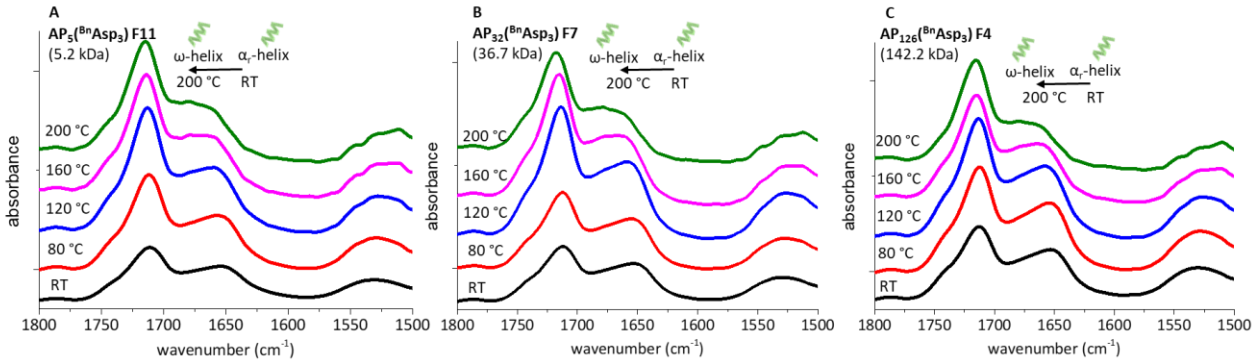

Figure S22. Temperature dependent FTIR measurement of A) **$AP_5(^{Bn}Asp_3)$ (F11)** (5.2 kDa), B)) **$AP_{32}(^{Bn}Asp_3)$ (F7)** (36.7 kDa) and C)) **$AP_{126}(^{Bn}Asp_3)$ (F4)** (142.2 kDa) at room temperature (RT, black curve), 80 °C (red curve), 120 °C (blue curve), 160 °C (pink curve) and 200 °C (green curve).

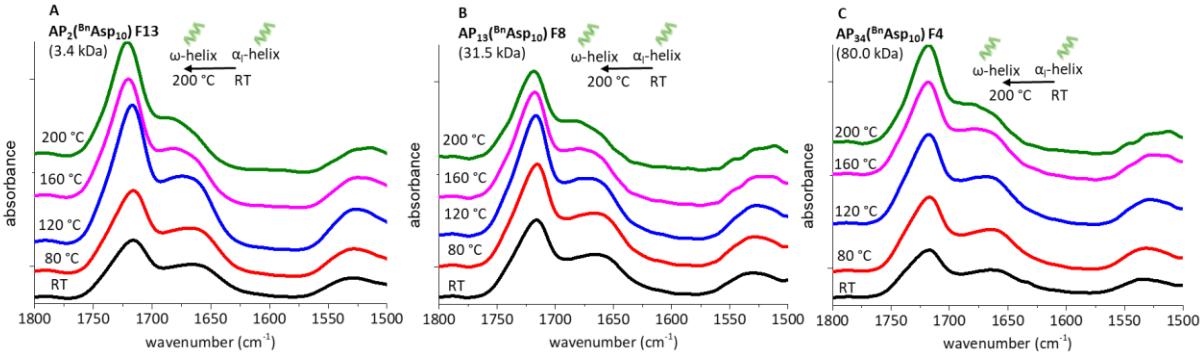

Figure S23. Temperature dependent FTIR measurement of A) **$AP_2(^{Bn}Asp_{10})$ (F13)** (3.4 kDa), B)) **$AP_{13}(^{Bn}Asp_{10})$ (F8)** (31.5 kDa) and C)) **$AP_{34}(^{Bn}Asp_{10})$ (F4)** (80.0 kDa) at room temperature (RT, black curve), 80 °C (red curve), 120 °C (blue curve), 160 °C (pink curve) and 200 °C (green curve).

S24. CD measurement of oligomer $O^{Bn}Glu_{10}$ and polymer $AP_3(^{Bn}Glu_{10})$ (unfractionated) in HFIP-solution.

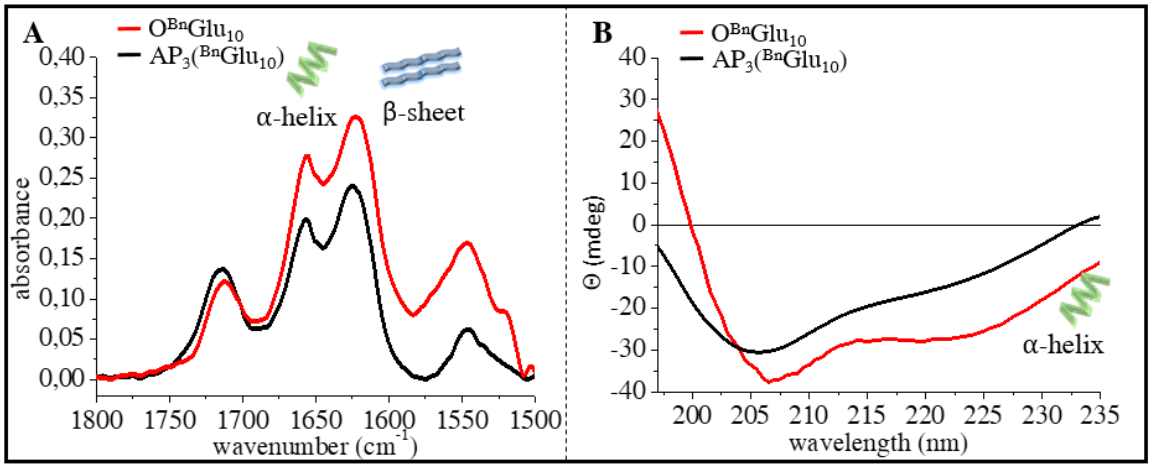

Figure S24. FTIR spectra (A) of the amide I and amide II region at concentrations of 2.0 mg mL^{-1} and CD spectra (B) at 0.2 mg mL^{-1} in HFIP for: **$O^{Bn}Glu_{10}$** (red) and **$AP_3(^{Bn}Glu_{10})$** (black).

S25. – S28. Concentration dependent FTIR measurements of oligomers and corresponding ADMET-polymers (unfractionated) in HFIP-solution.

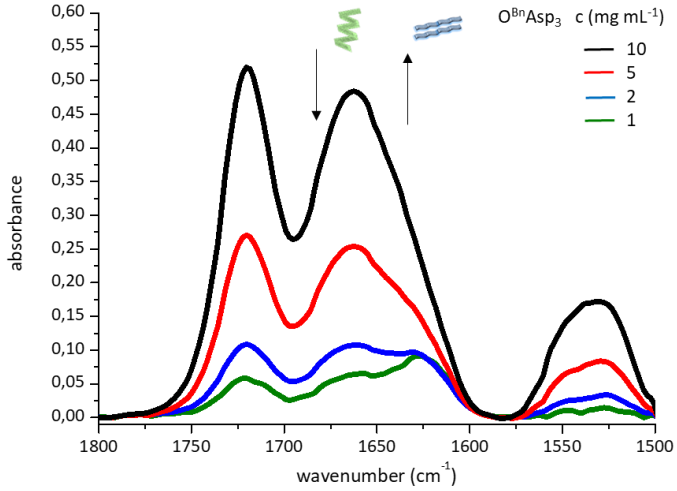

Figure S25. Concentration dependent measurement for **$O^{Bn}Asp_3$** at 10 mg mL^{-1} (black), 5mg mL^{-1} (red), 2 mg mL^{-1} (blue) and 1 mg mL^{-1} (green) with 0.5 mm PTFE spacer. With decreasing concentration an increasing amount of β-sheet structure could be observed.

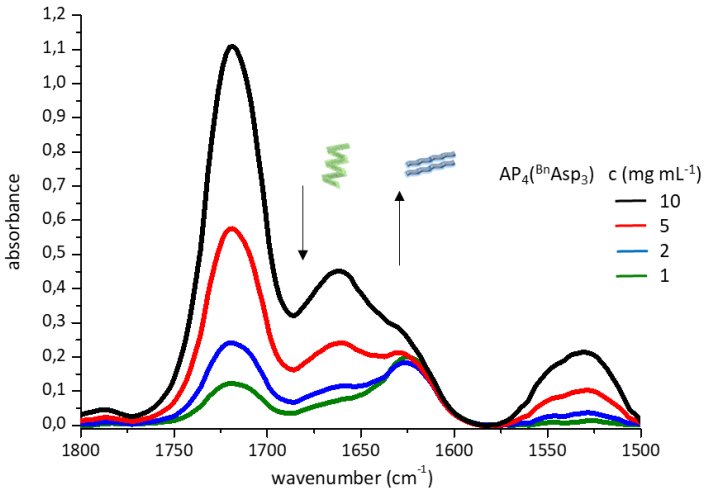

Figure S26. Concentration dependent measurement for **AP$_4$(^{Bn}Asp$_3$)** at 10 mg mL^{-1} (black), 5mg mL^{-1} (red), 2 mg mL^{-1} (blue) and 1 mg mL^{-1} (green) with 0.5 mm PTFE spacer. Mentioned that with decreasing concentration an increasing amount of β-sheet structure could be observed.

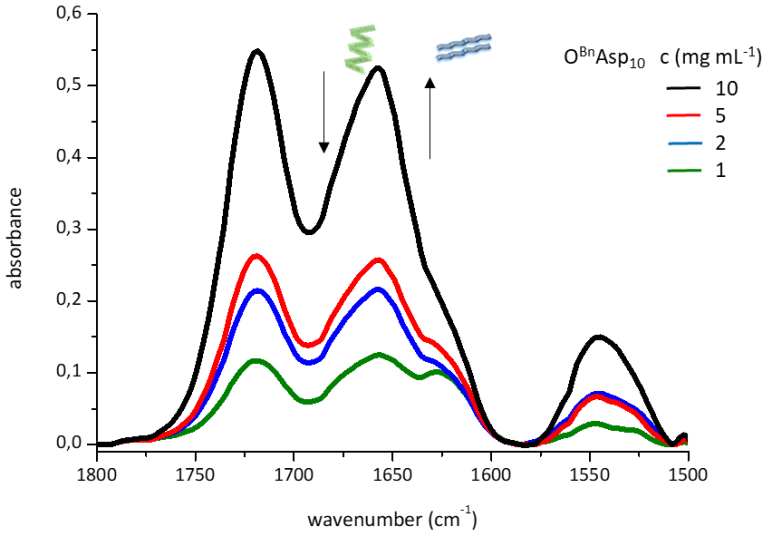

Figure S27. Concentration dependent measurement for **O^{Bn}Asp$_{10}$** at 10 mg mL^{-1} (black), 5mg mL^{-1} (red), 2 mg mL^{-1} (blue) and 1 mg mL^{-1} (green) with 0.5 mm PTFE spacer. Mentioned that with decreasing concentration an increasing amount of β-sheet structure could be observed.

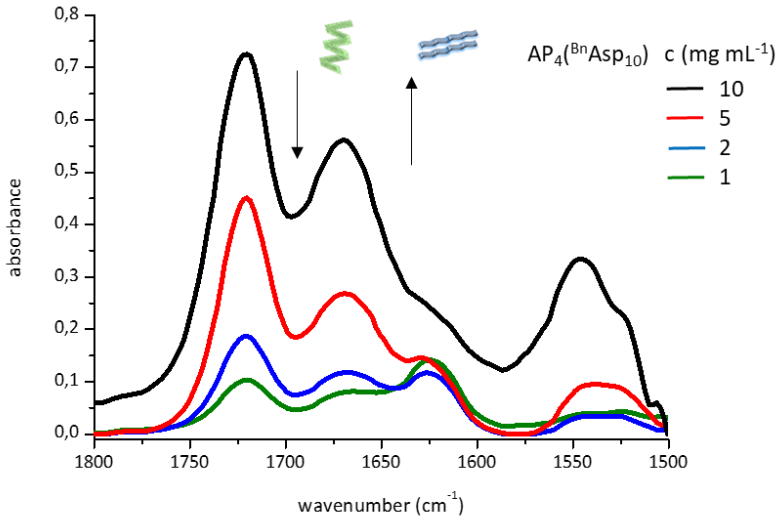

Figure S28. Concentration dependent measurement for **$AP_4(^{Bn}Asp_{10})$** at 10 mg mL^{-1} (black), 5mg mL^{-1} (red), 2 mg mL^{-1} (blue) and 1 mg mL^{-1} (green) with 0.5 mm PTFE spacer. Mentioned that with decreasing concentration an increasing amount of β-sheet structure could be observed.

References

1 K. M. Lambert, J. M. Bobbitt, S. A. Eldirany, L. E. Kissane, R. K. Sheridan, Z. D. Stempel, F. H. Sternberg and W. F. Bailey, *Chem. Eur. J*, 2016, **22**, 5156-5159.

1. G. J. M. Habraken, K. H. R. M. Wilsens, C. E. Koning and A. Heise, *Polym. Chem.*, 2011, **2**, 1322.